Solutes Alter the Conformation of the Ligand Binding Loops in Outer Membrane Transporters†

Miyeon Kim, Qi Xu,‡ David Murray, and David S. Cafiso*

Department of Chemistry and Biophysics Program, P.O. Box 400319, McCormick Road, University of Virginia, Charlottesville, Virginia

Received August 14, 2007; Revised Manuscript Received November 8, 2007

ABSTRACT: The binding and recognition of ligands by bacterial outer membrane transport proteins is mediated in part by interactions made through their extracellular loops. Here, site-directed spin labeling (SDSL) and electron paramagnetic resonance (EPR) spectroscopy were used to examine the effect of stabilizing solutes on the extracellular loops in BtuB, the vitamin B_{12} transporter, and FecA, the ferric citrate transporter. EPR spectra from the extracellular loops of FecA and BtuB arise from dynamic backbone segments, and distance measurements made by double electron−electron resonance indicate that the second extracellular loop in BtuB samples a wide range of conformations. These conformations are dramatically restricted upon substrate binding. In addition, the EPR spectra from nitroxide labels attached to the extracellular loops in BtuB and FecA are highly sensitive to solutes, and at every site examined the motion of the label is significantly reduced in the presence of stabilizing osmolytes, such as polyethylene glycols. For the second extracellular loop in BtuB, the solute-induced structural changes are small, but they are sufficient to bring spin-labeled side chains into tertiary contact with other portions of the protein. The spectroscopic changes seen by SDSL suggest that high concentrations of stabilizing solutes, such as those used to generate membrane protein crystals, result in a more compact and ordered state of the protein than is seen under more physiological conditions.

Bacterial outer membrane proteins are one of the best-studied classes of membrane proteins. In addition to porins and other passive transport proteins, the outer membrane includes a class of active transport proteins that function in the high-affinity binding and uptake of rare nutrients into the periplasmic space. These transport proteins are termed TonB-dependent, because they extract energy from the inner membrane proton potential by coupling to the transperiplasmic protein TonB (*1*). High-resolution structural models have been obtained by protein crystallography for a number of TonB-dependent transporters, including the iron transporters, FecA, FhuA, FepA, FptA, and FpvA (*2*−*7*), and the vitamin B_{12} transporter, BtuB (*8*, *9*). These proteins are all based upon a 22-stranded β-barrel, where the interior of the barrel is occluded by approximately 140−160 residues near the N-terminus. Large extracellular loops that link the β-strands in TonB-dependent transporters function to bind ligand and also form the receptor binding sites for colicins (*10*−*13*). On the periplasmic surface, a highly conserved region near the N-terminus termed the Ton box is thought to be responsible for coupling the transporter to TonB.

X-ray crystallography has been an invaluable tool for investigating TonB-dependent transport; nonetheless, the structural models that are obtained can be influenced by the conditions used to produce protein crystals. In BtuB, site-directed spin labeling (SDSL)[1] and electron paramagnetic resonance (EPR) spectroscopy indicate that the N-terminal Ton box undergoes a substrate-dependent conformational transition to generate an unfolded or disordered protein segment (*14*, *15*). Distance measurements made using pulse EPR indicate that this structural transition extends the Ton box 20−30 Å into the periplasmic space (*16*). This substrate-dependent unfolding of the Ton box is not observed by X-ray crystallography. Rather, the Ton box remains folded within the barrel of BtuB upon the addition of substrate. This discrepancy appears to result from the different solute conditions used in the spectroscopic and crystallographic approaches. Specifically, the high concentrations of salts and polyethylene glycols (PEGs) that are used for protein crystallization act to stabilize the folded form of the Ton box and effectively block this substrate-induced transition (*17*, *18*).

Solutes or osmolytes have a remarkable range of effects on protein structure (*19*−*23*). Osmolytes may unfold a protein, stabilize the native protein fold, or have no effect on protein stability. Solutes that denature proteins, such as urea and guanidinium, interact with the protein backbone

† This work was supported by a Grant from the National Institutes of Health, NIGMS, GM 035215.

* To whom correspondence should be addressed. E-mail: cafiso@virginia.edu. Phone: 434-924-3067. Fax: 434-924-3567.

‡ Present address: Epic Therapeutics, Inc., 220 Norwood Park South, Norwood, MA 02062.

[1] Abbreviations: DEER, double electron−electron resonance; EPR, electron paramagnetic resonance; L no., extracellular loop number; MOMD, microscopic order macroscopic disorder; MPD, 2-methyl-2,4-pentanediol; MTSL, methanethiosulfonate spin label; OG, *n*-octyl-β-D-glucopyranoside; PEG, poly(ethylene glycol); POPC, palmitoyloleoylphosphatidylcholine; R1, spin-labeled side chain produced by derivatization of a cysteine with the MTSL; SDSL, site-directed spin labeling; TMAO, trimethylamine *N*-oxide.

10.1021/bi7016415 CCC: $40.75
Published on Web 12/20/2007

and deplete water from regions near the protein surface. Osmolytes that tend to stabilize the native state of the protein (sugars, TMAO, polyols) are generally excluded from the protein surface so that the protein is preferentially hydrated in solutions of these solutes (*22*). Solutes may be excluded from a protein surface by several mechanisms. For example, the higher molecular weight PEGs are thought to be excluded by a steric mechanism or excluded volume (*24*), and they have been used to probe volume changes in proteins (*25*). The smaller naturally occurring osmolytes, such as TMAO, are excluded because they interact unfavorably with the protein backbone (*26*). Solutions of stabilizing osmolytes, such as PEGs and MPD (2-methyl-2,4-pentanediol), increase the free energy of proteins and make proteins less soluble, thus acting as effective precipitants for protein crystallization. However, proteins that exhibit a conformational equilibrium may be driven to a less hydrated, more folded state in the presence of these stabilizing osmolytes. In the case of BtuB, the conformational equilibrium exhibited by the Ton box is shifted toward its less hydrated, more folded state in the presence of the solutes used for protein crystallization (*18*).

At the present time, the effects of osmolytes on the dynamics or structure of the extracellular loops that link the β-strands in TonB-dependent transporters are unknown. Such effects might be large, due to the large solvent-accessible surface area of this region. These loops are typically well-resolved in protein crystal structures; although in the case of BtuB, the extracellular loops that connect strands 3−4 (L2), 5−6 (L3), and 7−8 (L4) are not fully resolved until vitamin B_{12} and its coligand Ca^{2+} are bound (*8*). In FepA, and FecA, there is evidence from chemical cross-linking (*27*) and X-ray crystallography (*3*), respectively, that there are large movements in the extracellular loops upon ligand binding. In FecA, the binding of ferric citrate induces changes of 11 and 15 Å in the position of the extracellular loops connecting strands 13 and 14 (L7), and 15 and 16 (L8), respectively (*3*). These loop movements may have several roles; for example, they may mediate signal transduction events within the protein that take place upon the binding of ligand, or they may function to close the loops around the ligand binding site to prevent ligand release back into the extracellular medium during the transport process. It has also been suggested that the closing of these loops may decrease bacterial susceptibility to colicins (*28*).

In the present work, the spin-labeled side chain R1 (see Figure 1a) was incorporated into the ligand binding loops of BtuB and FecA to explore the dynamics of the loops and to investigate the effects of stabilizing solutes such as PEGs on the loop structure and dynamics. Our data indicate that these extracellular loops are highly dynamic; but in every case examined, moderate concentrations of PEGs dramatically alter the EPR spectra from labeled sites in these loops so that these labels become more ordered in the presence of the solute. These spectroscopic changes are linearly dependent upon solute activity and indicate that the dynamics and conformation of these loops are highly sensitive to the solution environment. The results suggest that the presence of these solutes at high concentrations leads to a subset of protein conformational states that are more compact and more ordered than typically seen under more physiological conditions.

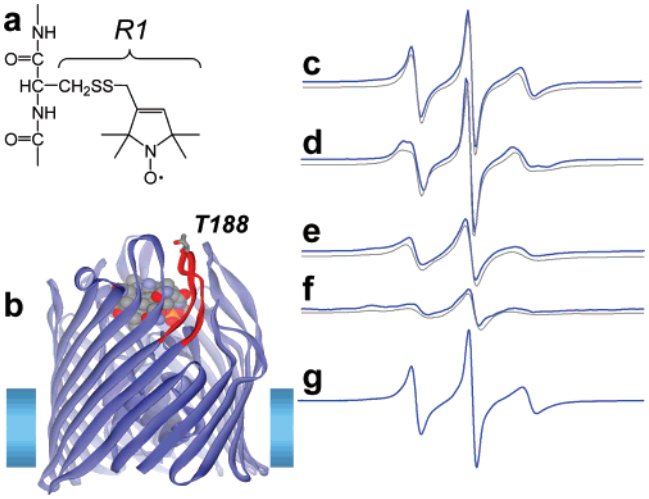

FIGURE 1: (a) Structure of spin-labeled side chain R1. (b) Molecular model obtained by X-ray crystallography for BtuB in the presence of Ca^{2+} and B_{12} (PDB ID: 1NQH) showing the position of T188 located in the second extracellular loop of BtuB, which connects β-strands 3 and 4, and normalized X-band EPR spectra obtained from T188R1. Spectra in (c) POPC in EPR buffer (220 mmol/kg), (d) plus Ca^{2+}/B_{12} (1.4 mM Ca^{2+} and 300 μM B_{12}), (e) plus crystal soaking solution, (f) plus Ca^{2+}/B_{12} and crystal soaking solution, and (g) plus 20% w/v Ficoll 400. The gray traces in spectra c−f are spectral simulations using the MOMD model (see text).

EXPERIMENTAL PROCEDURES

Mutagenesis, Protein Expression, and Outer Membrane Preparation. In order to attach a sulfhydryl-reactive spin label, a single cysteine mutation was introduced into BtuB (pAG1) (*29*) and FecA (pIS711) (*30*) wild-type plasmids using the QuickChange site-directed mutagenesis kit (Stratagene, La Jolla, CA). BtuB plasmids were transformed into an *E. Coli* RK5016 strain (*31*) for overexpression, whereas FecA was overexpressed in an *E. Coli* BL21(DE3) strain lacking all the outer membrane porins such as OmpA, OmpC, and LamB (*32*). Since this BL21(DE3) strain contains the phage T7 RNA polymerase on the chromosome under the control of the lacUV5 promoter, the transcription of FecA was initiated by the addition of 0.5 mM of isopropyl-β-D-thiogalactoside (IPTG). For BtuB expression, cells were grown in minimal "A" media supplemented with 0.2% glucose, 3 mM $MgSO_4$, 300 μM $CaCl_2$, and required amino acids 0.01% of Met and Arg, whereas FecA was expressed in LB media. Outer membrane was prepared as reported previously (*33*).

Purification, Spin Labeling, and Liposome Reconstitution. The isolated outer membrane was solubilized using the detergent, *n*-octyl-β-D-glucopyranoside (OG), ANAGRADE (Anatrace, Maumee, OH) in 100 mM Tris buffer (pH 8.05) containing 0.2 mM DTT and 5 mM EDTA. After centrifugation at 100 000*g* for 1 h, the solubilized protein in OG micelles remained in the supernatant and was spin-labeled by adding 1-oxyl-2,2,5,5-tetramethyl-3-pyrroline-3-methyl methanethiosulfonate (MTSL, Toronto Research Chemicals, North York, ON, Canada). The reaction mixture was incubated overnight in the dark at room temperature. Spin-labeled samples were then loaded onto a prepacked 5 mL Q-sepharose high-performance column (Amersham Biosciences, Piscataway, NJ), and a gradient was run from 0.25 to 1 M of LiCl in 25 mM BisTris buffer containing 17 mM OG (pH 7.0). Following purification, protein purity was

examined by SDS−PAGE electrophoresis, and the fractions containing pure BtuB and FecA were pooled and incubated with 1-palmitoyl-2-oleoyl-*sn*-glycero-3-phosphocholine (POPC, Avanti Polar Lipids, Alabaster, AL) and OG followed by reconstitution into liposomes. Reconstitution was achieved by removal of detergent from lipid−detergent mixed micelles using 10 kD MWCO Spetra/Por CE dialysis membranes (Rancho Dominguez, CA) (*34*). Mutants were dialyzed against 10 mM HEPES, 130 mM NaCl, 0.25 mM NaN_3, 1 μM EDTA, pH 6.5 for 3 days for reconstitution into POPC vesicles. The reconstituted vesicles were collected by centrifugation and further concentrated using a Beckman Airfuge.

Electron Paramagnetic Resonance Measurements. SDSL is a powerful method to explore local protein structure and backbone dynamics. Here, continuous wave EPR spectroscopy on the R1-labeled and reconstituted BtuB or FecA was performed on 4−5 μL of protein sample, which was loaded into a glass capillary with 0.60 mm i.d. × 0.84 mm o.d. (VitroCom, Mountain Lakes, NJ). EPR spectra were obtained using a Varian E-line 102 series X-band spectrometer fitted with a loop−gap resonator (Medical Advances, Milwaukee, WI). All spectra were taken at 2 mW incident microwave power and 1 G modulation amplitude and were normalized to the area under the absorption curve. For EPR measurements in the presence of vitamin B_{12} and $CaCl_2$, stock solutions were added directly to the reconstituted liposomes, which were taken through five times of freeze−thaw cycles using liquid N_2. Individual samples were prepared for titration experiments with PEG 3350 by mixing the appropriate amount of a 50% w/v PEG 3350 stock solution and EPR reconstitution buffer while maintaining the same concentration of protein. These samples were also taken through five freeze−thaw cycles. For measurements made in the crystallization solutions (*35*), the solutions were first dried using a Savant speed vac (Holbrook, NY) and then mixed with the protein sample to an equivalent volume. These samples were micellar and were not taken through freeze−thaw cycles.

The second moments of the EPR spectra were calculated using a LabView program (National Instruments, Austin, TX) provided by Dr. Christian Altenbach (UCLA), which implements a second-moment calculation described previously (*36*). Experimental EPR spectra were fit to the microscopic order macroscopic disorder (MOMD) model developed by Budil et al. using a modified Levenberg−Marquardt algorithm (*37*) in a manner similar to that described previously (*38*). Unless otherwise noted, tensor parameters were fixed to those used previously for surface-exposed R1 sites, with $A_{xx} = 6.2$, $A_{yy} = 5.9$, $A_{zz} = 37$, $g_{xx} = 2.0076$, $g_{yy} = 2.0050$, and $g_{zz} = 2.0023$, and the diffusion tilt parameters were set with $\alpha_D = 4$, $\beta_D = 36$, and $\gamma_D = 0$. In these simulations, S defines an order parameter, which represents the magnitude of a simple axially symmetric restoring potential used in the simulation (S is defined as $S = {}^1/_2\langle(3\cos^2\theta - 1)\rangle$, θ is the angle between the protein fixed director and the z-axis of the diffusion tensor, and the brackets indicate a spatial average).

Distance Measurements and Data Analysis by Pulse EPR. Four-pulse DEER measurements were performed with a Bruker Elexsys 580 spectrometer equipped with a 2 mm split-ring resonator under conditions of strong overcoupling (Q = 200) as described previously (*16*). The measurements were performed at approximately 80 K. The pulse sequence $(\pi/2)_{\nu 1} - \tau_1 - (\pi)_{\nu 1} - t' - (\pi)_{\nu 2} - \tau_1 + \tau_2 - t' - (\pi)_{\nu 1} - \tau_2 -$ echo was used with $\tau_1 = 200$ ns and $\tau_2 = 1200$ ns. The timing of the pump pulse was incremented by $\Delta t = 4$ ns, and an eight-step phase cycle was applied during data collection. The observe frequency ν_1 (typically 9.46 GHz) was set to the center of the resonator mode, with the static magnetic field set to the global maximum of the nitroxide spectrum. The pump frequency ν_2 (typically $\nu_2 - \nu_1 = 72$ MHz) was set to the local maximum at the low-field edge of the spectrum. Accumulation times for the data sets varied between 19 and 22 h. The dipolar time evolution data ($t = t' - \tau_1 > 0$) of double spin-labeled BtuB were analyzed using the MatLab program package DeerAnalysis 2006, provided by G. Jeschke (http://www.mpip-mainz.mpg.de/~jeschke/distance.html). The background contribution to the DEER signal was fitted with a two-dimensional distribution (planar background correction) corresponding to $\exp(-kt^{2/3})$, and the data were fit to either one or two Gaussian distance distributions.

Pulse experiments to determine the transverse relaxation time, or T2, of single nitroxide-labeled BtuB at 80 K were carried out using a standard Hahn echo with the pulse sequence $(\pi/2)_\nu - \tau - (\pi)_\nu - \tau -$ echo. Here, τ was set to 96 ns and incremented in 8 ns steps with 16 and 32 ns $\pi/2$ and π pulse lengths, respectively, and ν was set to the center of the resonator mode. Two-step phase cycling was used with a shot repetition time of 1020 μs.

Solute Activity and Free Energy Changes. The EPR spectra change as a function of solution osmolality, and we assume that this reflects a change in a conformational equilibrium within the protein. The conformational shift appears to involve the conversion from a more dynamic state to a less dynamic, more ordered state, and one may define an equilibrium constant, K, which is given by the ratio of the populations between two states so that $K = N_{\text{dynamic}}/N_{\text{ordered}}$.

In order to obtain the equilibrium constant, K, it was assumed that the EPR spectra, which varied as a function of solution osmolality, were a composite of two spectra arising from two distinct conformational states. The equilibrium constant for the conformation change at a particular site was determined from the EPR spectra as described previously-(*18*) and is expected to have the following behavior:

$$-\frac{\partial \ln K}{\partial \pi} = \frac{m}{kT} \tag{1}$$

where m is a parameter that reflects the free energy change per molal of solute activity and π is the solution osmotic pressure. Solute activity or solution osmolalities were measured using a Wescor 5500 vapor pressure osmometer (Logan, UT), and m was determined by linear extrapolation of a plot of $-\ln K$ versus the solution osmolality.

RESULTS

Extracellular Loops in BtuB Are Flexible and Become More Ordered upon Addition of Solutes. Spin labels were engineered into the extracellular loops of BtuB to probe changes in the dynamics and structure of this region of the protein. Shown in parts c and d of Figure 1 are EPR spectra of a nitroxide label in the apex of loop 2, T188R1, (linking β-strands 3 and 4) in the absence and presence of Ca^{2+}/B_{12},

respectively. The spectrum for T188R1 is narrow, and the nitroxide magnetic interactions are highly averaged, indicating that the label at this site is highly mobile. This spectrum is typical of an R1 side chain that is attached to a flexible loop site in a protein (*39*). In the presence of the BtuB substrate, vitamin B_{12} and its coligand Ca^{2+}, the EPR spectrum broadens, indicating that there is a decrease in motion of T188R1. A more quantitative estimate of the motion executed by these nitroxides can be obtained by simulating the EPR spectrum in the context of the MOMD model for nitroxide motion (see Experimental Procedures). In the absence of substrate, the spectrum from T188R1 can be fit adequately using a single component with isotropic motion corresponding to correlation time of approximately 1.4 ns, although acceptable fits can also be obtained with slightly faster rates and small non-zero-order parameters (*S* values less than 0.1). Upon the addition of substrate, the spectrum can be also be fit with a single motional component having a correlation time of 1.2 ns and an order parameter of approximately 0.33, with acceptable fits being obtained for *S* in the range of 0.29−0.35. It has been shown that backbone dynamics is an important component in determining EPR line shapes (*40*), and if the change seen between parts c and d of Figure 1 is due entirely to a change in backbone motion, it would indicate a reduction in the rms angle of backbone motion of approximately 10−15°.

Previously, it was observed that solutes that stabilize protein structure, such as PEGs, effectively block the substrate-induced conformational change in the Ton box of BtuB (*17*, *18*). This conformational change involves a change in hydration, and these solutes lower the energy of the less hydrated protein conformation relative to the more hydrated form. Since the extracellular loops in BtuB and other outer membrane transporters are highly hydrated, we examined these loops in the presence of solutes typically used to produce protein crystals to determine whether their structure or dynamics was sensitive to these stabilizing solutes. Shown in parts e and f of Figure 1 are normalized spectra for T188R1 in the presence of the crystallization soaking solution (*35*) without and with Ca^{2+}/vitamin B_{12}, respectively. One of the major solutes contributing to the osmolality of this solution is PEG 3350, and solutions of this solute alone will also produce the changes seen in Figure 1, parts e and f (see below). The EPR spectra in the presence of the crystallization solution are dramatically broadened and are characteristic of nitroxides that are in tertiary contact. With the use of the MOMD model, these spectra could be fit with two motional components, one with highly isotropic motion and a correlation time of 2− 3 ns, and a second that is highly ordered and effectively near the rigid limit on the EPR time scale.

In general, a broadening of the EPR line shape might result from the increased viscosity of the crystallization soaking solutions. To test for this possibility we recorded the spectrum of T188R1 in a 20% w/v solution of Ficoll 400, a 400 000 molecular weight polymer which has approximately the same viscosity as a 30% w/v solution of PEG 3350 but with an osmolality (solute activity) which is similar to that of the typical buffer used here for EPR (10 mM HEPES, 130 mM NaCl, pH 6.5). The spectrum obtained in Ficoll 400 for T188R1 in the absence of ligand is shown in Figure 1g. It is virtually identical to that seen in Figure 1c, indicating that the label motion is unchanged from that seen for the

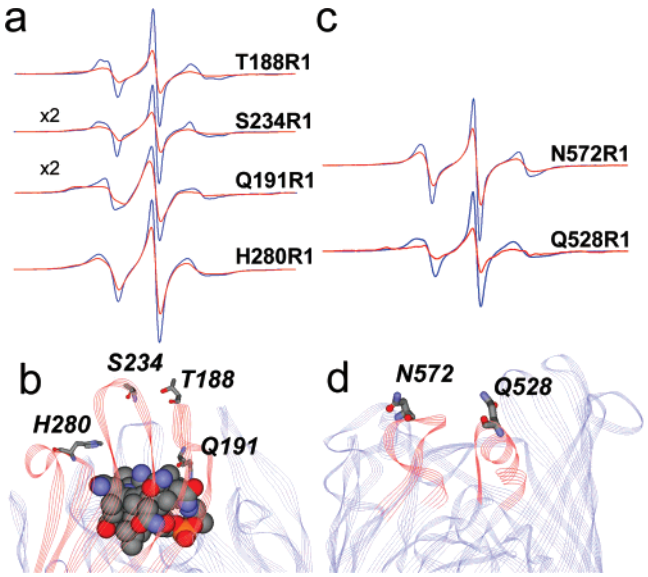

FIGURE 2: (a) EPR spectra of BtuB with Ca^{2+} and B_{12} in POPC (blue) or the spectra in the presence of approximately 30% PEG 3350 (red): T188R1 and Q191R1 in the second extracellular loop, S234R1 in the third extracellular loop, and H280R1 in the fourth extracellular loop. Spectral amplitudes are normalized against the total spin number. (b) Molecular model obtained by crystallography for BtuB showing sites that were spin labeled in the second, third, and fourth extracellular loops (PDB ID: 1NQH). (c) EPR spectra of FecA in POPC (blue) or in the presence of approximately 30% w/v PEG 3350 (red). N572R1 is at the apex of the eighth loop linking β-strands 15 and 16, Q528R1 is on the final turn of a helix that forms part of the seventh loop and links β-strands 13 and 14. (d) Molecular model obtained by crystallography for FecA showing sites that were labeled in the seventh and eighth loops (PDB ID: 1KMO).

protein in POPC with the EPR buffer. Thus, solution viscosity does not make a major contribution to the line shape changes seen in the crystallization solution, and the results suggest that a different property of the solution, such as solute activity or solution osmolality, may be responsible for the reduction in motional averaging that is seen in the nitroxide EPR spectrum.

In addition to T188R1, spin labels were placed into a number of sites in the extracellular binding loops of BtuB. Shown in Figure 2a are EPR spectra from Q191R1 in loop 2, S234R1 in loop 3, and H280R1 in loop 4 (Figure 2b). The spectra were taken in the presence of substrate, in an EPR buffer (blue traces), or in 30% PEG 3350 (red traces). At every site, 30% PEG 3350 produces a change in the EPR spectrum that corresponds to an increase in ordering and/or decrease in rate of motion of the nitroxide.

The effects of solutes such as PEGs are not limited to the extracellular loops of BtuB. Shown in Figure 2c are EPR spectra, in the absence of substrate, for N572R1 in loop 8 and Q528R1 in loop 7 of the ferric citrate transporter FecA (Figure 2d). Under conditions of low osmolality, the EPR spectrum from the label at N572R1 is consistent with a label placed into a flexible loop. Q528R1 is located on the terminal turn of a helix positioned in loop 7, and the line shape from this label is very similar to those found previously for exposed sites on a flexible helix (*38*, *41*). In the presence of 30% w/v PEG 3350, the spectra broaden, indicating that both these labels have undergone a significant decrease in motional averaging. The spectrum observed for N572R1 in the presence of PEG does not have obvious broad features

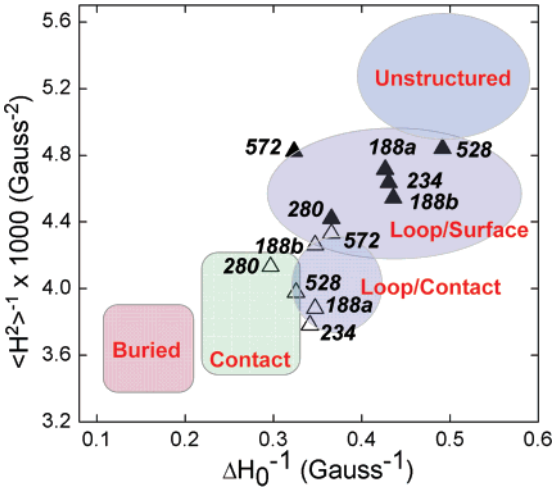

FIGURE 3: Plot of the reciprocal of the central line width (ΔH_0^{-1}) vs the reciprocal of the second moment ($\langle H^2 \rangle^{-1}$) of the EPR spectrum for sites in the extracellular loops of BtuB and FecA in the absence (▲) and presence (△) of 30% w/v PEG 3350. Two sets of points are shown for BtuB T188R1: 188a is in the presence of substrate (vitamin B_{12} + Ca^{2+}) and 188b is in the absence of substrate.

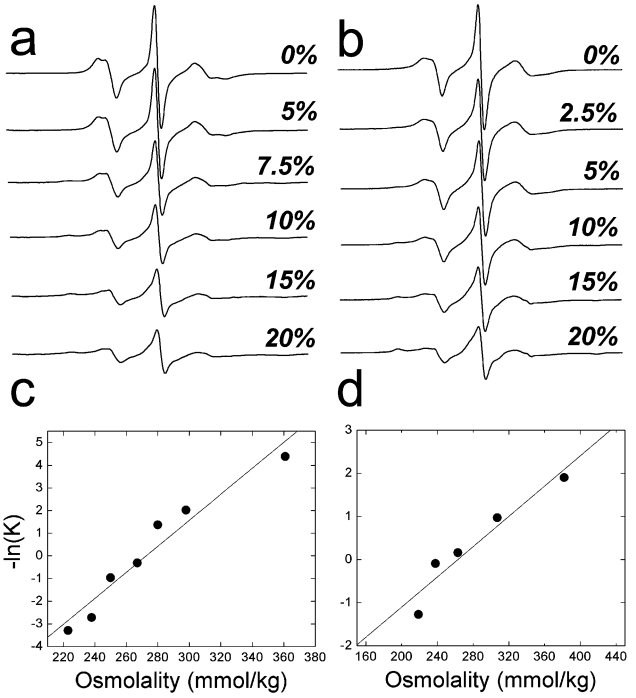

FIGURE 4: EPR spectra of (a) BtuB T188R1 and (b) FecA Q528R1 in POPC at PEG 3350 concentrations ranging from 0% to 20% w/v. Addition of the PEG results in a conversion of the EPR spectrum to one that arises from a more immobile nitroxide. Plots of ln(*K*) vs osmolality of PEG 3350 obtained for (c) BtuB T188R1 and (d) FecA Q528R1. Here, if the spectra from T188R1 and Q528R1 are assumed to arise from two states, *K* represents the equilibrium constant between the two states.

that would indicate the development of label tertiary contact (*39*), and therefore this broadened spectrum may result from an increase in backbone ordering. The broad spectral features that appear for Q528R1 in the presence of PEG indicate that a structural change has taken place that brings this side chain into tertiary contact with other portions of FecA.

The second moment, $\langle H^2 \rangle$, and central resonance line width, ΔH_0, of an R1 spectrum are parameters that provide a qualitative characterization of the protein structure at the labeled site (*39*). The central line width is dominated by the label correlation time, whereas the second moment is influenced both by correlation time and by the label ordering (*41*). A reciprocal plot of the second moment and central line width are shown in Figure 3 for spectra from T188R1, H280R1, S234R1, N572R1, and Q528R1 in the absence (filled symbols) and presence (open symbols) of 30% PEG 3350. In the absence of PEG, these EPR spectra reflect those typically obtained at exposed loop or helix surface sites. In the presence of PEG 3350, the parameters from these EPR spectra indicate that the labels are undergoing slower motion, and each label (with the exception of N572R1) is now characteristic of a spectrum obtained for a label in tertiary contact.

Extracellular Loops in BtuB and FecA Are Modulated by Solute Activity. The EPR spectra for labels in BtuB and FecA (Figure 2) were recorded as a function of PEG 3350 concentration. Figure 4a shows a series of spectra obtained from the BtuB label T188R1 in the presence of 0−20% PEG. Figure 4b shows spectra from the FecA label Q528R1 as a function of the concentration of PEG 3350. For each label, EPR spectra broaden progressively as the concentration of PEG 3350 is increased, and spectra from the two sites (particularly T188R1) are quite sensitive to even low percentages of this solute.

Each of the spectra in Figure 4, parts a and b, may be reproduced by summing the appropriate populations of the two limiting spectra (at zero and the highest concentrations of PEG 3350 used). If the structural changes that are giving rise to these spectra are assumed to result from two conformational states, the equilibrium partitioning between these two states can be determined (*18*) (see Experimental Procedures). Parts c and d of Figure 4 are plots of the natural logarithm of the apparent equilibrium constant *K* as a function of osmolality for T188R1 and Q528R1. Each of the plots are linear, indicating that the apparent free energy associated with this conformational change is linearly dependent upon solute activity. When expressed as a free energy change per molal of solute activity, the slopes of the lines in Figure 4, parts c and d, yield values of approximately 35 and 13 kcal/mol, respectively. For T188R1, the sensitivity to solute activity is quite dramatic, and it is approximately 10-fold larger than that seen previously for the substrate-induced unfolding transition in the Ton box (see Table 1) (*18*). Q191R1 is also located on the second extracellular loop, and a plot of ln(*K*) versus osmolality for this label (data not shown) yields a plot with approximately the same slope as that seen for T188R1. A reasonable explanation for the similar slopes for T188R1 and Q191R1 is that both spin labels are monitoring the same conformation change that occurs with solute addition.

The EPR spectra obtained for other labeled sites in BtuB and FecA were examined as a function of the concentration of PEG 3350, and Table 1 lists values for free energy changes that are estimated for the labeled sites in BtuB and FecA. For comparison, Table 1 also lists the conformational energy shift found previously using PEG 3350 for the Ton box in BtuB (this was obtained previously from a label at position 10 in the Ton box, V10R1). The free energy changes seen in the loop regions with equivalent concentrations of PEG 3350 are approximately 3−9 times larger than that seen in the Ton box (*18*), and there is considerable variability

Table 1: Conformational Free Energy Change Per Molal of Solute Activity

	spin label		solute	ΔG (kcal/mol)[a]
BtuB	Ton box	V10R1	PEG 3350	4.0
	extracellular loops	T188R1	PEG 3350	34
		S234R1	PEG 3350	33
		H280R1	PEG 3350	16
		T188R1	PEG 400	1.4
		T188R1	glycine betaine	0.2
FecA	extracellular loops	Q528R1	PEG 3350	13
		N572R1	PEG 3350	14

[a] Errors in the free energies based upon the standard deviations obtained from multiple measurements are estimated to be approximately ±20%.

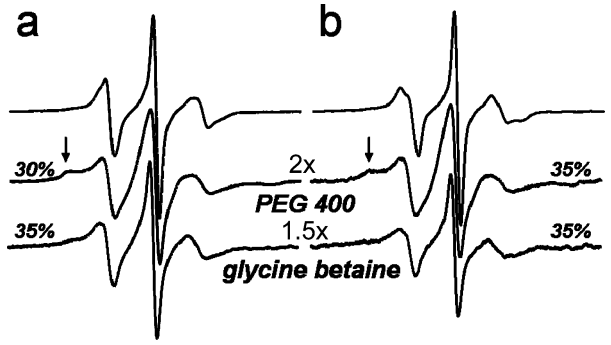

FIGURE 5: X-band EPR spectra of BtuB T188R1 in POPC (a) without and (b) with the substrate vitamin B_{12} and its coligand, Ca^{2+}. The top spectrum is obtained for the sample in EPR buffer. The two spectra below are obtained in the presence of the stabilizing osmolytes PEG 400 and glycine betaine at the given percentage concentrations (w/v). The *y*-axes for the spectra in PEG 400 and glycine betaine are enlarged by factors of 2 and 1.5, respectively, relative to the sample in POPC. The arrows indicate the position of immobilized components that appear in these spectra. Scans are 100 G.

between the loops. The labeled site in loop 3, S234R1, yields a sensitivity to solutes that is similar to that seen for Q191R1 and T188R1 in loop 2. The value for H280R1 in loop 4 and the values obtained for the two labeled sites in FecA are considerably smaller. In general, the sensitivity of these loop sites roughly correlates with the size of the extracellular loop and the solvent-accessible surface area (SASA) for the loop seen in the protein crystal structures (BtuB SASA: loop 2 > loop 3 > loop 4). Although a precise molecular interpretation cannot be made from these data, the results indicate that loop conformations in BtuB and FecA are modulated by solute activity.

Smaller solutes that act as protein stabilizers also produce changes in the EPR spectra from the R1-labeled loop sites in BtuB and FecA. Shown in Figure 5 are EPR spectra of T188R1 in the absence or presence of PEG 400 and glycine betaine. As seen for PEG 3350, the spectra from T188R1 broaden in glycine betaine and PEG 400, indicating that there is a reduction in the motional averaging of the nitroxide. The spectra also exhibit a broad component that arises from the label coming into tertiary contact. However, when these spectra are examined as a function of solute activity, the sensitivity of these spectral changes to solute is dramatically reduced compared to PEG 3350 (see Table 1). This result is not unexpected, and it is consistent with the idea that the larger PEGs are more excluded from the hydrated protein surface due to steric effects (*22*, *42*, *43*).

Distance Measurements Define Ligand and Solute-Induced Structural Changes in BtuB. The data presented in Figures 2 and 4 and Table 1 indicate that large apparent energy differences are associated with PEG 3350 induced conformational changes in BtuB and FecA; however, these data do not provide an indication of the size of these structural changes or where within these membrane proteins the structural changes originate. Conceivably, changes in the dynamics or structure of the BtuB or FecA loops upon PEG addition might be the result of protein aggregation, leading to changes in the EPR spectra of labels attached to these loops. Solutes such as PEG are precipitants, and they might alter the lateral distribution of the protein within the bilayer. However, two experiments performed here argue against this possibility. First, aggregation of BtuB within the bilayer was monitored by measuring the T2 or spin−spin relaxation rate of T188R1 at 80 K using a simple Hahn echo (see Experimental Procedures). This relaxation rate is highly sensitive to local protein concentration and protein aggregation, and T2 will dramatically shorten upon aggregation. Measurements of T188R1 in POPC yielded a T2 time of about 1.8 μs, which increased slightly to 2 μs in the presence of 30% (w/v) PEG 3350. This result indicates that aggregation of BtuB is not taking place with the addition of this solute. Second, when these transporters were solubilized in an OG detergent micelle under very dilute conditions, the EPR spectra showed changes upon the addition of PEG 3350 that were similar to those seen in POPC. The fact that similar changes in the EPR spectra are seen whether the protein is present in membranes or solubilized in detergent also argues against a PEG-induced change in the aggregation state of the protein.

The EPR spectra from T188R1 (Figure 1) indicate that the second extracellular loop in BtuB is highly dynamic and that addition of ligand reduces this motion. Furthermore, the EPR spectra from T188R1 are consistent with a PEG 3350 induced structural change in loop 2 that places the R1 label at this site into tertiary contact. To probe the size of the ligand and PEG-induced structural changes in this portion of BtuB, pairs of labels were engineered into BtuB where one nitroxide was located at position 188 on the apex of loop 2 and a second label was placed at one of three positions within the BtuB barrel, see Figure 6, parts a and b. A pulse EPR technique, double electron−electron resonance (DEER) (*44*), was then used to measure weak dipolar couplings between the two labels, which were used to estimate distances and distributions of distances between the labels (see Experimental Procedures).

Shown in Figure 6c are DEER data for the spin-labeled pair T188R1/G399R1 that have been background subtracted. Also shown are fits (red traces) to the data using a Gaussian distance distribution. The distances corresponding to these fits are given in Table 2. The protein in its apo form in POPC gives rise to a highly dampened DEER signal, indicating that there is a broad distance distribution between these nitroxides. Similar signals are seen for the two other mutant pairs T188/D291 and T188/N488 (Figure 6, parts d and e) when BtuB is in its apo form. The standard deviation in the Gaussian fits to these distributions is greater than 10 Å. Upon

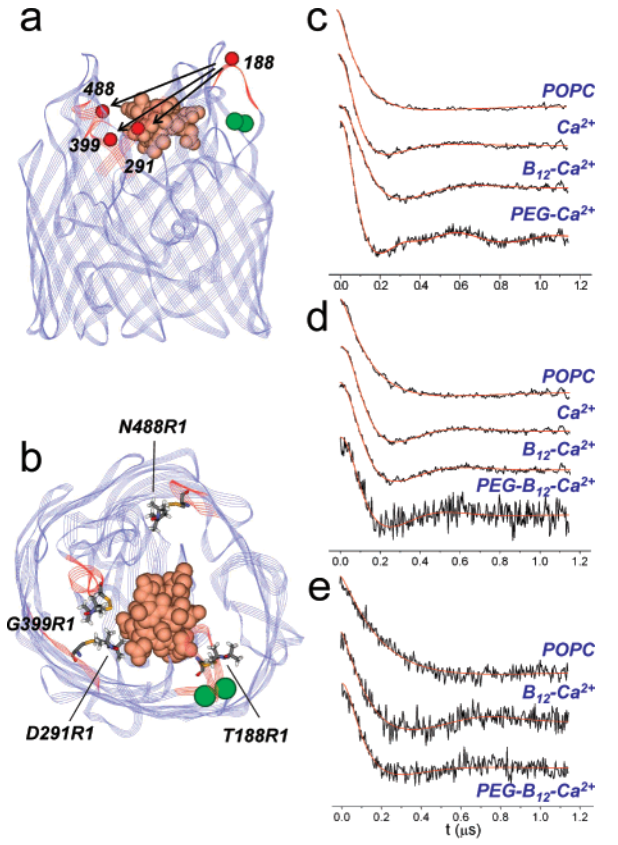

FIGURE 6: Distance measurements in BtuB. (a) Structure of BtuB (PDB ID: 1NQH) showing the Cα carbons of T188, D291, G399, and N488, which have been mutated in pairs to cysteine for incorporation of the spin-labeled side chain R1. (b) Top view of the spin-labeled side chain R1 when incorporated into the positions indicated in part a. T188R1 is in the apex of loop 2, D291 is on the inward-facing side of strand 8 near loop 4, G399R1 is on a helical turn in loop 7, and N488R1 is on the inward-facing side of loop 9. Vitamin B_{12} is rendered as a CPK structure, Ca^{2+} ions are in green. (c) DEER signals obtained for T188R1/G399R1 reconstituted into POPC in the apo form, with Ca^{2+}, with Ca^{2+} and vitamin B_{12}, and with Ca^{2+} and 30% w/v PEG 3350. (d) DEER signals obtained for T188R1/D291R1 in the apo form, with Ca^{2+}, with Ca^{2+} and vitamin B_{12}, and with Ca^{2+} and vitamin B_{12} and 30% w/v PEG 3350. (e) DEER signals obtained for T188R1/N488R1 in the apo form, with Ca^{2+} and vitamin B_{12}, and with Ca^{2+} and vitamin B_{12} and 30% w/v PEG 3350.

the addition of Ca^{2+}, or Ca^{2+} and vitamin B_{12}, oscillations are seen in the DEER for each mutant pair indicating that the distance distributions have narrowed. For T188R1/G399R1 the distributions narrow from 11 to less than 6 Å, and similar changes are seen in the other two mutant pairs. In the presence of PEG 3350, the data for T188R1/G399R1 is fit well by two Gaussian distributions, where the major population has a mean distance that is more than 2 Å shorter than the sample lacking PEG. This difference appears to be significant, as judged by uncertainty in the Gaussian fits and reproducibility in the sample data. Slightly shorter distances are also seen for the T188R1/D291R1 and T188R1/N488R1 labeled pairs, but the DEER data for these mutants is noisier than that for T188R1/G399R1, and the differences are within experimental error.

The data shown in Figure 6 indicate that distances to the spin label in the second extracellular loop in BtuB undergo large fluctuations, which are attenuated upon the binding of ligand. The EPR spectra for the single-labeled sites, G399R1, D291R1, and N488R1 (spectra not shown), do not change upon the addition of substrate or Ca^{2+}, and although the EPR line shape of T188R1 changes, it does not come into tertiary contact upon the addition of these ligands. As a result, changes in the rotameric states of the spin label, which involve the conformation of the linkage to the protein backbone, are unlikely to be the source of these distance changes. Rather, the most likely explanation for the decrease in distance distribution with substrate addition is a change in conformation and/or dynamics of the second extracellular loop. It should be noted that the mean distances measured by DEER in the presence of substrate are roughly consistent with the Cα distances based upon the crystal structure (*8*) and the likely rotameric states of the spin-labeled side chain.

DISCUSSION

The extracellular loops in TonB-dependent transporters are involved in the high-affinity binding of trace nutrients, such as iron chelates and vitamin B_{12}. The EPR spectra obtained here for nitroxides attached to the loop regions of BtuB or FecA indicate that these regions of the protein are highly mobile on the nanosecond time scale. In the case of BtuB, loops near the ligand binding site become more ordered upon the binding of ligand, and distance measurements to the second loop in BtuB indicate that large structural fluctuations are dramatically suppressed when Ca^{2+} and vitamin B_{12} bind. These results are qualitatively consistent with the results of crystallography (*8*), which fail to resolve loops 2−4 in the apo form of BtuB but resolve these loops when vitamin B_{12} and Ca^{2+} are bound. Chemical cross-linking (*27*), fluorescence quenching (*45*), and X-ray crystallography (*3*) of FecA also indicate that substrate binding can have dramatic effects on loop dynamics or structure. These changes are not unexpected, as a reduction in protein dynamics following binding is often observed for regions of proteins that interact with ligands (*46*−*48*) or with other proteins (*49*).

High solute concentrations are well-known to have a range of effects on proteins. For example, protein stability is seen to increase in the presence of some solutes, whereas others can drive the folding of unfolded proteins. (*22*, *50*−*53*). Solutes are also known to modulate protein conformational changes in ion channels, hemoglobin, and enzymes (*25*, *43*, *54*, *55*). In BtuB, previous work demonstrated that the substrate-induced undocking of the Ton box was modulated by solutes and that solute effects accounted for the discrepancy between crystallographic and spectroscopic measurements in this protein (*17*, *18*).

In the presence of high concentrations of PEG 3350, the motion of nitroxides at sites in the extracellular loops of both BtuB and FecA decreased in every case examined. At the majority of these sites, PEG 3350 addition also brought the nitroxide label into tertiary contact at the labeled site. DEER measurements on the second extracellular loop of BtuB indicated that there were small movements of this protein segment with the addition of this PEG 3350. The mostly likely interpretation of these data is that PEG addition promotes a compaction of this loop but does not profoundly alter the loop structure. The changes in the EPR spectra shown in Figures 1 and 2 might be due to a direct binding of PEG and other solutes to the labeled loop sites. This would explain both the tertiary contact of the label (T188R1) in

Table 2: Mean Distances and Distributions in angstroms Obtained from DEER Data[a]

BtuB sample	T188R1/G399R1	T188R1/D291R1	T188R1/N488R1
POPC, apo	29.8 ± 11	32 ± 11	36 ± 13
Ca^{2+}	27.5 ± 5.4	29.3 ± 4.5	
Ca^{2+}, vitamin B_{12}	30.7 ± 4.6	29.4 ± 4.5	29.8 ± 7.6
Ca^{2+}, PEG 3350	24.9 ± 3 (67%) 29.9 ± 4.6 (33%)		
Ca^{2+}, B_{12}, PEG 3350	27.9 ± 5 (76%) 29.7 ± 1 (24%)	28.5 ± 3.8	28.9 ± 6.7

[a] The DEER data in Figure 6 were fit to Gaussian distributions using the MatLab program package DeerAnalysis 2006 (see Experimental Procedures) to yield a mean distance and a distance distribution. The distribution represents a standard deviation of the Gaussian. In two cases, more than one Gaussian was necessary to obtain a fit to the data, and for these cases, the numbers in parenthesis indicate the fraction of spins in each distance distribution. On the basis of repeated measurements and fits of both identical and different samples, the uncertainty in the mean distances is estimated to be approximately 1−2 Å with the spin concentrations and experimental parameters used here. Errors in the distance distributions are approximately 20%.

the presence of PEG and the relatively small distance changes (Figure 6). However, this is not a behavior that has been reported for PEGs (which are generally believed to be excluded from protein surfaces (*22*)). It is also not consistent with the use of PEGs as precipitants, and it does not explain why the effect of PEG 3350 should roughly track with the solvent-accessible surface area of the BtuB and FecA loops. When taken together with the known effect of PEGs on proteins, the data suggest that these solutes result in a compaction of the extracellular region of BtuB and that the modest structural changes, which take place in loop 2 with PEG addition, must be large enough to hinder the motion of the nitroxide label. At the present time, we do not know whether other extracellular loops in BtuB or FecA will show similar or larger distance changes when compared to those seen in loop 2 of BtuB.

Polyethylene glycols are thought to precipitate proteins and stabilize proteins because they are sterically excluded from regions around the protein surface (*22*). The exclusion of this solute from the protein, and the preferential hydration of the protein, raise the free energy of the protein in the solution (*42*). This increase in energy will tend to precipitate the protein from solution. However, if an equilibrium exists between protein conformations of differing hydration, the addition of PEGs to the solution will tend to stabilize the less hydrated conformation, because the energy of this conformation will be lowered relative to the more hydrated form (*19*, *20*). In the case of PEGs, the degree of exclusion (and preferential hydration) increases with the increase in PEG molecular weight indicating that the principle source of this preferential hydration is steric exclusion (*42*). The data obtained here are generally consistent with this conclusion. For example, PEG 3350 was observed to have a much larger effect than either PEG 400 or glycine betaine. The concept of steric exclusion is also consistent with the rough correlation seen between the solvent-exposed surface area of the extracellular loop and the magnitude of the free energy changes shown in Table 1.

Solutions typically utilized for protein crystallization often employ high concentrations of PEGs and salts as precipitants. The data presented here on the ordering of the BtuB and FecA transporter loops by PEG 3350 indicate that the crystal structures of these TonB-dependent transporters likely display a higher level of order and a conformation that is on average more compact than that seen under more physiological conditions. As indicated above, there is a large body of work demonstrating that osmolytes modulate protein stability; however, there are relatively few examples demonstrating molecular level changes with solutes like PEGs or illustrating how PEGs could influence the models generated by protein crystallography. In hexokinase, PEG effects on the activity of the enzyme indicate the protein explores a wider range of hydrated states in solution than is seen in the crystal structure (*54*). In the membrane protein bacteriorhodopsin, there is evidence that altered hydration or altered ionic strength leads to changes in the structure of the protein within the crystal (*56*). And in the Ton box of FecA, there is evidence that the structure of this segment of the transporter is modified by solutes that are typically used for protein crystallization (*57*).

In summary, the data presented here indicate that the extracellular loops in BtuB and FecA are dynamic and that they can undergo significant changes in structure upon ligand binding. Stabilizing osmolytes, such as PEGs, produce dramatic changes in the EPR spectra obtained from nitroxides in these loops. In the second extracellular loop of BtuB, the structural changes produced by PEG are relatively small but indicate that this region becomes more compact and ordered in the presence of these solutes. The work suggests that the structures of dynamic regions of membrane proteins that undergo changes in hydration may be strongly influenced by protein-stabilizing solutes.

ACKNOWLEDGMENT

We thank Dr. Volkmar Braun (University of Tübingen, Germany) for the FecA strain and plasmid, Drs. Wayne Hubbell, and Christian Altenbach (UCLA) for LabView software used in the EPR data analysis, and Dr. Michael Wiener (University of Virginia) for providing crystallization solutions. We also thank Dr. Steven Lukasik for his assistance in recording DEER spectra.

REFERENCES

1. Postle, K., and Kadner, R. (2003) Touch and go: tying TonB to transport, *Mol. Microbiol. 49*, 869−882.
2. Ferguson, A. D., Chakraborty, R., Smith, B. S., Esser, L., Van der Helm, D., and Deisenhofer, J. (2002) Structural basis of gating by the outer membrane transporter FecA, *Science 295*, 1715−1719.
3. Yue, W. W., Grizot, S., and Buchanan, S. K. (2003) Structural evidence for iron-free citrate and ferric citrate binding to the TonB-dependent outer membrane transporter FecA, *J. Mol. Biol. 332*, 353−368.

4. Ferguson, A. D., Hofmann, E., Coulton, J. W., Diederichs, K., and Welte, W. (1998) Siderophore-mediated iron transport: crystal structure of FhuA with bound lipopolysaccharide, *Science 282*, 2215−2220.
5. Buchanan, S. K., Smith, B. S., Venkatramanil, L., Xia, D., Esser, L., Palnitkar, M., Chakraborty, R., van der Helm, D., and Deisenhofer, J. (1999) Crystal structure of the outer membrane active transporter FepA from *Escherichia coli*, *Nat. Struct. Biol. 6*, 56−63.
6. Cobessi, D., Celia, H., and Pattus, F. (2005) Crystal structure at high resolution of ferric-pyochelin and its membrane receptor FptA from *Pseudomonas aeruginosa*, *J. Mol. Biol. 352*, 893−904.
7. Cobessi, D., Celia, H., Folschweiller, N., Schalk, I. J., Abdallah, M. A., and Pattus, F. (2005) The crystal structure of the pyoverdine outer membrane receptor FpvA from *Pseudomonas aeruginosa* at 3.6 angstroms resolution, *J. Mol. Biol. 347*, 121−134.
8. Chimento, D. P., Mohanty, A. K., Kadner, R. J., and Wiener, M. C. (2003) Substrate-induced transmembrane signaling in the cobalamin transporter BtuB, *Nat. Struct. Biol. 10*, 394−401.
9. Cherezov, V., Yamashita, E., Liu, W., Zhalnina, M., Cramer, W. A., and Caffrey, M. (2006) In meso structure of the cobalamin transporter, BtuB, at 1.95 A resolution, *J. Mol. Biol. 364*, 716−734.
10. Kurisu, G., Zakharov, S. D., Zhalnina, M. V., Bano, S., Eroukova, V. Y., Rokitskaya, T. I., Antonenko, Y. N., Wiener, M. C., and Cramer, W. A. (2003) The structure of BtuB with bound colicin E3 R-domain implies a translocon, *Nat. Struct. Biol. 10*, 948−954.
11. Killmann, H., Videnov, G., Jung, G., Schwarz, H., and Braun, V. (1995) Identification of receptor binding sites by competitive peptide mapping: phages T1, T5, and phi 80 and colicin M bind to the gating loop of FhuA, *J. Bacteriol. 177*, 694−698.
12. Newton, S. M., Allen, J. S., Cao, Z., Qi, Z., Jiang, X., Sprencel, C., Igo, J. D., Foster, S. B., Payne, M. A., and Klebba, P. E. (1997) Double mutagenesis of a positive charge cluster in the ligand-binding site of the ferric enterobactin receptor, FepA, *Proc. Natl. Acad. Sci. U.S.A. 94*, 4560−4565.
13. Jiang, X., Payne, M. A., Cao, Z., Foster, S. B., Feix, J. B., Newton, S. M. C., and Klebba, P. E. (1997) Ligand-specific opening of a gated-porin channel in the outer membrane of living bacteria, *Science 276*, 1261−1264.
14. Merianos, H. J., Cadieux, N., Lin, C. H., Kadner, R., and Cafiso, D. S. (2000) Substrate-induced exposure of an energy-coupling motif of a membrane transporter, *Nat. Struct. Biol. 7*, 205−209.
15. Fanucci, G. E., Coggshall, K. A., Cadieux, N., Kim, M., Kadner, R. J., and Cafiso, D. S. (2003) Substrate-induced conformational changes of the perplasmic N-terminus of an outer-membrane transporter by site-directed spin labeling, *Biochemistry 42*, 1391−1400.
16. Xu, Q., Ellena, J. F., Kim, M., and Cafiso, D. S. (2006) Substrate-dependent unfolding of the energy coupling motif of a membrane transport protein determined by double electron−electron resonance, *Biochemistry 45*, 10847−10854.
17. Fanucci, G. E., Lee, J. Y., and Cafiso, D. S. (2003) Spectroscopic evidence that osmolytes used in crystallization buffers inhibit a conformation change in a membrane protein, *Biochemistry 42*, 13106−13112.
18. Kim, M., Xu, Q., Fanucci, G. E., and Cafiso, D. S. (2006) Solutes modify a conformational transition in a membrane transport protein, *Biophys. J. 90*, 2922−2929.
19. Parsegian, V. A., Rand, R. P., and Rau, D. C. (2000) Osmotic stress, crowding, preferential hydration, and binding. A comparison of perspectives, *Proc. Natl. Acad. Sci. U.S.A. 97*, 3987−3992.
20. Timasheff, S. N. (2002) Protein hydration, thermodynamic binding, and preferential hydration, *Biochemistry 41*, 13473−13482.
21. Timasheff, S. N. (2002) Protein−solvent preferential interactions, protein hydration, and the modulation of biochemical reactions by solvent components, *Proc. Natl. Acad. Sci. U.S.A. 99*, 9721−9726.
22. Bolen, D. W. (2004) Effects of naturally occurring osmolytes on protein stability and solubility: issues important in protein crystallization, *Methods 34*, 312−322.
23. Rosgen, J., Pettitt, B. M., and Bolen, D. W. (2007) An analysis of the molecular origin of osmolyte-dependent protein stability, *Protein Sci. 16*, 733−743.
24. Arakawa, T., and Timasheff, S. N. (1985) Mechanism of poly-(ethylene glycol) interaction with proteins, *Biochemistry 24*, 6756−6762.
25. Zimmerberg, J., Bezanilla, F., and Parsegian, V. A. (1990) Solute inaccessible aqueous volume changes during opening of the potassium channel of the squid giant axon, *Biophys. J. 57*, 1049−1064.
26. Street, T. O., Bolen, D. W., and Rose, G. D. (2006) A molecular mechanism for osmolyte-induced protein stability, *Proc. Natl. Acad. Sci. U.S.A. 103*, 13997−4002.
27. Scott, D. C., Newton, S. M., and Klebba, P. E. (2002) Surface loop motion in FepA, *J. Bacteriol. 184*, 4906−4911.
28. Postle, K. (2002) Close before opening, *Science 295*, 1658−1659.
29. Gudmundsdottir, A., Bell, P. E., Lundrigan, M. D., Bradbeer, C., and Kadner, R. J. (1989) Point mutations in a conserved region (TonB box) of *Escherichia coli* outer membrane protein BtuB affect vitamin B12 transport, *J. Bacteriol. 171*, 6526−6533.
30. Kim, I., Stiefel, A., Plantor, S., Angerer, A., and Braun, V. (1997) Transcription induction of the ferric citrate transport genes via the N-terminus of the FecA outer membrane protein, the Ton system and the electrochemical potential of the cytoplasmic membrane, *Mol. Microbiol. 23*, 333−344.
31. Heller, K., Mann, B. J., and Kadner, R. J. (1985) Cloning and expression of the gene for the vitamin B12 receptor protein in the outer membrane of *Escherichia coli*, *J. Bacteriol. 161*, 896−903.
32. Prilipov, A., Phale, P. S., Van Gelder, P., Rosenbusch, J. P., and Koebnik, R. (1998) Coupling site-directed mutagenesis with high-level expression: large scale production of mutant porins from *E. coli*, *FEMS Microbiol. Lett. 163*, 65−72.
33. Coggshall, K. A., Cadieux, N., Piedmont, C., Kadner, R., and Cafiso, D. S. (2001) Transport-defective mutations alter the conformation of the energy-coupling motif of an outer membrane transporter, *Biochemistry 40*, 13946−13971.
34. Ollivon, M., Lesieur, S., Grabielle-Madelmont, C., and Paternostre, M. (2000) Vesicle reconstitution from lipid−detergent mixed micelles, *Biochim. Biophys. Acta 1508*, 34−50.
35. Chimento, D. P., Mohanty, A. K., Kadner, R. J., and Wiener, M. C. (2003) Crystallization and initial X-ray diffraction of BtuB, the integral membrane cobalamin transporter of *Escherichia coli*, *Acta Crystallogr. D59*, 509−511.
36. Slichter, C. P. (1978) *Principles of Magnetic Resonance*, 2nd ed., Springer-Verlag, Berlin, Heidelberg, New York.
37. Budil, D. E., Lee, S., Saxena, S., and Freed, J. H. (1996) Nonlinear-least-squares analysis of slow motion EPR spectra in one and two dimensions using a modified Levenberg−Marquardt algorithm, *J. Magn. Reson., Ser. A 120*, 155−189.
38. Columbus, L., Kalai, T., Jeko, J., Hideg, K., and Hubbell, W. L. (2001) Molecular motion of spin labeled side chains in α-helices: analysis by variation of side chain structure, *Biochemistry 40*, 3228−3846.
39. Mchaourab, H., Lietzow, M., Hideg, K., and Hubbell, W. (1996) Motion of spin-labeled side-chains in T4 lysozyme. (I) Correlation with protein structure and dynamics, *Biochemistry 35*, 7692−7704.
40. Columbus, L., and Hubbell, W. L. (2002) A new spin on protein dynamics, *Trends Biochem. Sci. 27*, 288−295.
41. Columbus, L., and Hubbell, W. L. (2004) Mapping backbone dynamics in solution with site-directed spin labeling: GCN4-58 bZip free and bound to DNA, *Biochemistry 43*, 7273−7287.
42. Bhat, R., and Timasheff, S. N. (1992) Steric exclusion is the principal source of the preferential hydration of proteins in the presence of polyethylene glycols, *Protein Sci. 1*, 1133−1143.
43. Vodyanoy, I., Bezrukov, S. M., and Parsegian, V. A. (1993) Probing alamethicin channels with water-soluble polymers. Size-modulated osmotic action, *Biophys. J. 65*, 2097−2105.
44. Pannier, M., Veit, S., Godt, A., Jeschke, G., and Spiess, H. W. (2000) Dead-time free measurement of dipole−dipole interactions between electron spins, *J. Magn. Reson. 142*, 331−340.
45. Cao, Z., Warfel, P., Newton, S. M. C., and Klebba, P. E. (2003) Spectroscopic observations of ferric enterobactin transport, *J. Biol. Chem. 278*, 1022−1028.
46. Doring, K., Surrey, T., Nollert, P., and Jahnig, F. (1999) Effects of ligand binding on the internal dynamics of maltose-binding protein, *Eur. J. Biochem. 266*, 477−483.
47. Williams, D. H., Zhou, M., and Stephens, E. (2006) Ligand binding energy and enzyme efficiency from reductions in protein dynamics, *J. Mol. Biol. 355*, 760−767.
48. Khajehpour, M., Wu, L., Liu, S., Zhadin, N., Zhang, Z. Y., and Callender, R. (2007) Loop dynamics and ligand binding kinetics in the reaction catalyzed by the Yersinia protein tyrosine phosphatase, *Biochemistry 46*, 4370−4378.

49. Dyson, H. J., and Wright, P. E. (2005) Intrinsically unstructured proteins and their functions, *Nat. Rev. Mol. Cell Biol. 6*, 197−208.
50. Mello, C. C., and Barrick, D. (2003) Measuring the stability of partly folded proteins using TMAO, *Protein Sci. 12*, 1522−1529.
51. Baskakov, I., Wang, A., and Bolen, D. W. (1998) Trimethylamine-*N*-oxide counteracts urea effects on rabbit muscle lactate dehydrogenase function: a test of the counteraction hypothesis, *Biophys. J. 74*, 2666−2673.
52. Baskakov, I., and Bolen, D. W. (1998) Forcing thermodynamically unfolded proteins to fold, *J. Biol. Chem. 273*, 4831−4834.
53. Qu, Y., Bolen, C. L., and Bolen, D. W. (1998) Osmolyte-driven contraction of a random coil protein, *Proc. Natl. Acad. Sci. U.S.A. 95*, 9268−9273.
54. Reid, C., and Rand, R. P. (1997) Probing protein hydration and conformational states in solution, *Biophys. J. 72*, 1022−1030.
55. Colombo, M. F., Rau, D. C., and Parsegian, V. A. (1992) Protein solvation in allosteric regulation: a water effect on hemoglobin, *Science 256*, 1335−1336.
56. Portuondo-Campa, E., Schenkl, S., Dolder, M., Chergui, M., Landau, E. M., and Haacke, S. (2006) Absorption spectroscopy of three-dimensional bacteriorhodopsin crystals at cryogenic temperatures: effects of altered hydration, *Acta Crystallogr., Sect. D: Biol. Crystallogr. 62*, 368−374.
57. Kim, M., Fanucci, G. E., and Cafiso, D. S. (2007) Substrate-dependent transmembrane signaling in TonB-dependent transporters is not conserved, *Proc. Natl. Acad. Sci. U.S.A. 104*, 11975−11980.

BI7016415